Gallery of Fluid Motion

Confined Rayleigh-Taylor instability

Samar Alqatari,[1] Thomas E. Videbæk,[2] Sidney R. Nagel,[1] Anette Hosoi,[3] and Irmgard Bischofberger[3]

[1]*Department of Physics, James Franck Institute, and Enrico Fermi Institute, University of Chicago, Chicago, Illinois 60637, USA*

[2]*Department of Physics, Brandeis University, Waltham, Massachusetts 02453, USA*

[3]*Department of Mechanical Engineering, Massachusetts Institute of Technology, Cambridge, Massachusetts 02139, USA*

(Received 17 June 2022; published 7 November 2022)

This paper is associated with a poster winner of a 2021 American Physical Society's Division of Fluid Dynamics (DFD) Milton van Dyke Award for work presented at the DFD Gallery of Fluid Motion. The original poster is available online at the Gallery of Fluid Motion, https://doi.org/10.1103/APS.DFD.2021.GFM.P0041.

DOI: 10.1103/PhysRevFluids.7.110504

The interface between two stratified layers of fluids is stable when the denser fluid is on the bottom. For the inverted situation, with the denser fluid on top, the tug of gravity acts to lower the potential energy by upending the layers. This is the familiar Rayleigh-Taylor instability that is ubiquitous across scales, from milk poured into coffee to exploding supernovae [1,2]. However, setting up the unstable situation with clean initial conditions can be experimentally challenging [3,4]. Here, to achieve controlled initial conditions, we take advantage of the inherent stratification of fluids formed by a different instability, the viscous fingering of miscible fluids in a confined geometry [5–7].

We use a horizontal Hele-Shaw geometry consisting of two circular glass plates of diameter 25 cm, separated by a thin uniform gap $b \sim 1$ mm [8]. After filling the space between the parallel plates with a viscous outer fluid, a lower-viscosity inner fluid is injected into this gap through a hole in the center of one plate. Because of the unfavorable viscosity contrast, local pressure gradients amplify small perturbations along the fluid interface creating long, wide fingers [5]. If the two fluids are miscible, the displacing inner fluid creates a tongue of three stratified layers in which the inner fluid is sandwiched between two layers of the outer one [9–11]. If the fluid densities are not identical, one of the two fluid interfaces will necessarily be density inverted, a situation ripe for the formation of Rayleigh-Taylor plumes.

Figure 1 shows a top view of one quadrant of the plates after a less-viscous inner fluid has been injected into a dyed outer fluid with which it is miscible. This forms the canonical viscous-fingering pattern with three vertically stratified layers inside the gap. Throughout the region displaced by the inner fluid, one can see intricate dark and bright cellular patterns due to the formation of plumes, sharp up- or downwelling of the interface. The two fluids are sufficiently viscous so that these Rayleigh-Taylor plumes occur only after the fluid injection has stopped. Figure 2 shows images from a confocal-microscope movie of a single plume as it grows. The plumes exhibit the classic

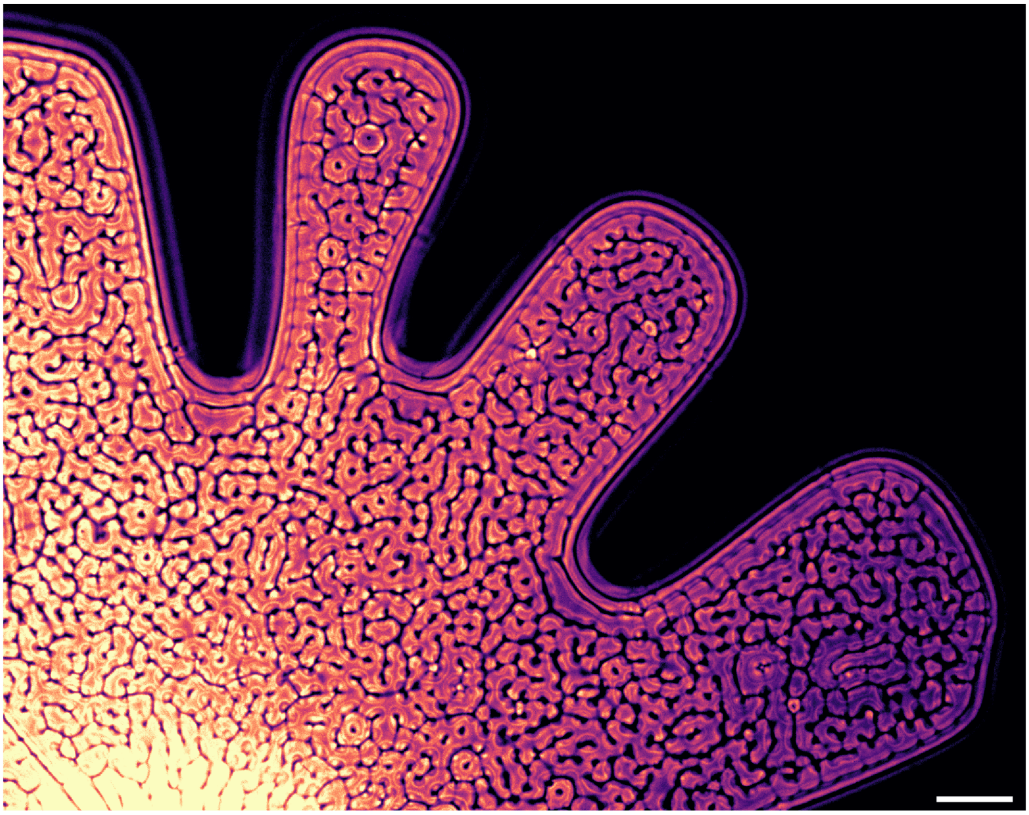

FIG. 1. Close-up image of the characteristic cellular patterns created by Rayleigh-Taylor plumes on a density-inverted stratified layer of fluids. The stratification is achieved during the formation of larger-scale viscous fingers of two miscible fluids. Plumes of the denser fluid sink and form convection rolls as they encounter the lower glass plate. The returning fluid, as it displaces the upper lighter layer of fluid, produces the thin bright lines visible inside the cells in the regions between the dark lines. The image is taken on a BW Prosilica GX3300 camera and lens with $f/32$ aperture. The original grayscale image has been colored to accentuate the finer details of the emergent pattern. The scale bar is 1 cm. The viscosity ratio between the fluids is $\eta_{\text{in}}/\eta_{\text{out}} \approx 0.03$ and the density difference is $\Delta\rho \approx 0.007$ g/ml. https://doi.org/10.1103/APS.DFD.2021.GFM.P0041.

Rayleigh-Taylor mushroom shape as they develop. At later times, diffusion between the two fluids erodes the sharp interfacial structure in the plumes, eventually causing the cellular pattern seen in Fig. 1 to fade.

By adjusting the control parameters (the plate spacing b and the densities and viscosities of the two fluids), we characterize the Rayleigh-Taylor instability and identify different regimes of confinement. We use various concentrations of glycerol-water mixtures to create a range of density contrasts between the pairs of fluids. The fraction of the gap occupied by each fluid can be determined from the measured transmitted light intensity. Using a two-dimensional Fourier transform of the patterns, we extract the dominant length scale, the instability wavelength λ. By varying the thickness of the gap between the plates b, we find that the instability is completely suppressed below a critical gap $b_c \sim (\eta D/g\Delta\rho)^{1/3}$, where g is the earth's gravitational constant. As b is increased, the instability changes from this mass-diffusion-dominated regime of stability, through an intermediate regime where the dynamics are set strictly by the gap $\lambda \sim b$, to the limit where the boundaries no longer affect the dynamics. In this last regime, the instability is governed by a competition between momentum diffusion and the unstable density gradient as predicted by

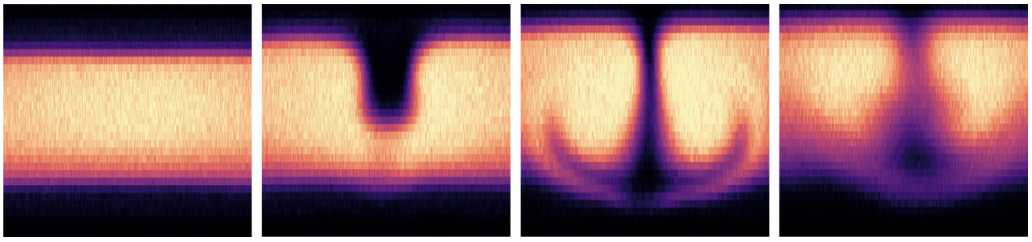

FIG. 2. Growth of a Rayleigh-Taylor plume in the thin gap of thickness $b = 1.14$ mm, imaged using a Caliber I.D. RS-G4 confocal microscope. To capture the dynamics of the instability we are limited to the number of z slices we can acquire, here 31. It is this reduced information in z that lends a pixelated quality to the image. The height of the images corresponds to the gap thickness b. The images are taken at times, from left to right, $t = 0, 330, 750, 1590$ s. The viscosities of the darker outer and the brighter inner fluids are $\eta_{\text{out}} = 610$ cP and $\eta_{\text{in}} = 101$ cP, respectively, and the effective interfluid diffusion coefficient is $D = 0.52 \times 10^{-6}$ cm^2/s. The density difference between the two fluids is $\Delta\rho = 0.031$ g/cm^3. Images in this figure are adapted from the original work [12]. https://doi.org/10.1103/APS.DFD.2021.GFM.P0041.

theory in the unconstrained limit $\lambda \sim (\nu D/gA)^{1/3}$, where $\nu = \eta/\rho$ is the kinematic viscosity and $A = \Delta\rho/\sum_i \rho_i$ is the nondimensional density contrast [12].

In our experiment, the Rayleigh-Taylor instability takes place on the back of the structure formed by the viscous-fingering instability of miscible fluids. We use one instability to probe another. The ephemeral appearance of internal features all across the horizontal interfaces can be easy to miss: They are visible only for a short time. They are literally the elegant shadows, the Platonic form if you will [13], of Rayleigh-Taylor plumes, one of the most fundamental of hydrodynamic instabilities.

This work made use of the shared facilities at the University of Chicago Materials Research Science and Engineering Center.

[1] J. S. Wettlaufer, The universe in a cup of coffee, Phys. Today **64**(5), 66 (2011).
[2] W. H. Cabot and A. W. Cook, Reynolds number effects on Rayleigh-Taylor instability with possible implications for type-Ia supernovae, Nat. Phys. **2**, 562 (2006).
[3] M. S. Roberts and J. W. Jacobs, The effects of forced small-wavelength, finite-bandwidth initial perturbations and miscibility on the turbulent Rayleigh-Taylor instability, J. Fluid Mech. **787**, 50 (2015).
[4] A. Aubertin, G. Gauthier, J. Martin, D. Salin, and L. Talon, Miscible viscous fingering in microgravity, Phys. Fluids **21**, 054107 (2009).
[5] P. Saffman and G. Taylor, The penetration of a fluid into a porous medium or Hele-Shaw cell containing a more viscous liquid, Proc. R. Soc. London Ser. A **245**, 312 (1958).
[6] L. Paterson, Fingering with miscible fluids in a Hele Shaw cell, Phys. Fluids **28**, 26 (1985).
[7] F. Haudin, L. A. Riolfo, B. Knaepen, G. M. Homsy, and A. de Wit, Experimental study of a buoyancy-driven instability of a miscible horizontal displacement in a Hele-Shaw cell, Phys. Fluids **26**, 044102 (2014).
[8] M. R. Wilson, Flow geometry controls viscous fingering, Phys. Today **65**(10), 15 (2012).
[9] E. Lajeunesse, J. Martin, N. Rakotomalala, and D. Salin, 3D Instability of Miscible Displacements in a Hele-Shaw Cell, Phys. Rev. Lett. **79**, 5254 (1997).
[10] I. Bischofberger, R. Ramachandran, and S. R. Nagel, Fingering versus stability in the limit of zero interfacial tension, Nat. Commun. **5**, 5265 (2014).
[11] T. E. Videbæk, Delayed onset and the transition to late time growth in viscous fingering, Phys. Rev. Fluids **5**, 123901 (2020).

[12] S. Alqatari, T. E. Videbæk, S. R. Nagel, A. E. Hosoi, and I. Bischofberger, Confinement-induced stabilization of the Rayleigh-Taylor instability and transition to the unconfined limit, Sci. Adv. **6**, eabd6605 (2020).

[13] S. R. Nagel, Shadows and ephemera, Crit. Inq. **28**, 23 (2001).